Journal of Power Sources 225 (2013) 226–230

Contents lists available at SciVerse ScienceDirect

Journal of Power Sources

journal homepage: www.elsevier.com/locate/jpowsour

Short communication

# Anomalous effect of K ion on crystallinity and capacitance of the manganese dioxide

Chunguang Wei [a,b], Chengjun Xu [a], Baohua Li [a], Hongda Du [a], Ding Nan [b], Feiyu Kang [a,b,*]

[a] City Key Laboratory of Thermal Management Engineering and Materials, Graduate School at Shenzhen, Tsinghua University, Shenzhen, Guangdong 518055, China
[b] State Key Laboratory of New Ceramics and Fine Processing, Department of Materials Science and Engineering, Tsinghua University, Beijing 100084, China

## HIGHLIGHTS

- Describe a fundamental study which correlates $K^+$ has the anomalous effect on $MnO_2$ crystalline state and capacitance.
- Adding $K^+$ not only delayed the conversion of $MnO_2$ crystalline, but also delayed the phase transformation temperature.
- The specific capacitance value big difference from 58 F $g^{-1}$ for H2/400 to 124 F $g^{-1}$ for K12/400.
- These results have important implications for the characterization of $MnO_2$ in catalysis and supercapacitor applications.

## GRAPHICAL ABSTRACT

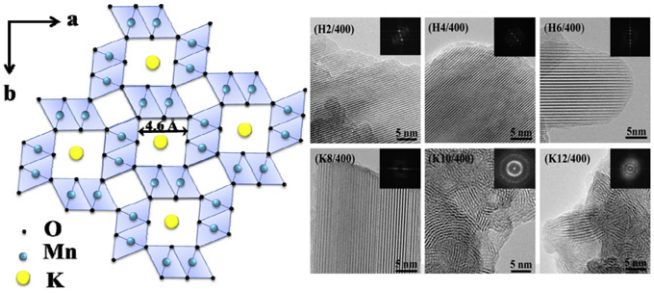


## ARTICLE INFO

*Article history:*
Received 14 August 2012
Received in revised form
17 September 2012
Accepted 19 September 2012
Available online 17 October 2012

*Keywords:*
Nanoparticles
Nanostructures
Amorphous
Supercapacitor

## ABSTRACT

A small amount of cations such as $Li^+$, $Na^+$, $K^+$, or $NH_4^+$ is required to stabilize the tunnels during the formation of $MnO_2$. Here, the effect of the content of K ion on crystalline state and capacitance behavior of $MnO_2$ are investigated. It is found that with the content of K ion increasing, manganese dioxide is more likely to maintain amorphous, while adding $Li^+$, $Na^+$, or $NH_4^+$ has no such effect. Adding K ion not only delays the conversion of manganese dioxide crystalline, but also delays the phase transformation temperature, which causes the big difference of specific capacitance value from 58 F $g^{-1}$ for H2/400 to 124 F $g^{-1}$ for K12/400. Furthermore, the morphology, special surface area, and pore data change dramatically from H2/400 to K12/400. These results have important implications for the characterization of $MnO_2$ in supercapacitor applications.



Manganese dioxide is of considerable importance in several industrial applications, such as catalysts, rechargeable batteries, molecular sieves due to its cheap, nontoxic, environmentally friendly and abundance of raw material, which has attracted interests for studies [1–8]. The basic crystal structure of manganese dioxide consists of $MnO_6$ octahedral units, which share vertices and edges to form tunnel structures [9,10]. Furthermore, changing valence state and various tunnel structure of $MnO_2$ result in ever-changing physical and chemical properties [11].

It has been shown that the properties of $MnO_2$ strongly depend on its powder dimension, morphology, crystalline, specific surface area, and bulk density [12–15], thus it is believed that the nanoscale structure design and synthesis of $MnO_2$ is the key point to

* Corresponding author. City Key Laboratory of Thermal Management Engineering and Materials, Graduate School at Shenzhen, Tsinghua University, Shenzhen, Guangdong 518055, China. Tel.: +86 755 2603 6188; fax: +86 (0)755 26036417.
*E-mail address:* fykang@tsinghua.edu.cn (F. Kang).

0378-7753/$ – see front matter 
http://dx.doi.org/10.1016/j.jpowsour.2012.09.076

improve its properties. And dimensionality, morphology and particle size of $MnO_2$ have been regarded as critical factors to its exciting physicochemical properties [16,17].

It is believed that a small amount of cations such as $Li^+$, $Na^+$, $K^+$, $NH_4^+$, or $H_3O^+$ is required to stabilize the tunnels in the formation of $MnO_2$ [18,19]. As well known, most methods to synthesize $MnO_2$ are based on the redox reactions of $Mn^{4+}$ and $Mn^{2+}$, and $KMnO_4$ is the most commonly used oxidant [20–23], as a result, the reaction product ($MnO_2$) usually contains K ion. However, studies on the role of K ion on the effect of manganese dioxide crystalline state remain rare. Here, we show an anomalous effect of K ion on the crystallinity and capacitance behavior of the manganese dioxide, which is different from the effect of $Li^+$, $Na^+$, and $NH_4^+$.

In this study, Amorphous $MnO_2$ samples with different contents of K ion are synthesized by using common liquid co-precipitation method based on the redox reactions of $Mn^{4+}$ and $Mn^{2+}$ at room temperature (RT). The content of K ion was controlled by using solution of KOH and HCl (see Supporting information). The sample so prepared was denoted as MX/Y, where M represents the type of acid or alkaline solution used, X represents the pH value of the reaction solution and Y represents the temperature of calcination. For example, H2, H4, H6, K8, K10 and K12 mean the product that the pH value of the reaction solutions is 2, 4, 6, 8, 10 and 12, respectively. And K8, Na8, NH8 and Li8 mean the products which use solution of KOH, NaOH, $NH_3 \cdot H_2O$, and LiOH to adjust the pH value of the reaction solutions to 8. While K8/400 means K8 sample was annealed at 400 °C.

The as-prepared $MnO_2$ powders are amorphous or poorly crystalline in nature. Fig. 1(a) shows the XRD patterns of the as-prepared samples at room temperature, it is clearly seen that at room temperature, when using LiOH, NaOH, $NH_3 \cdot H_2O$ instead of KOH to adjust the solution pH value, all the as-prepared samples are amorphous. The XRD patterns of as-prepared samples after annealing in air at 400 °C for 4 h are shown in Fig. 1(b). It is found that unlike other samples which grow into good crystalline, all of the diffraction peaks match with α-$MnO_2$ (JCPDS. No. 44-0141). After it is annealed at 400 °C, H2, H4, and H6 show good crystalline, while K8, K10 and K12 maintain their amorphous characteristics.

It should be pointed out that the K/Mn ratio of samples is almost unchanged at room temperature and after heat-treatment in air at 400 °C for 4 h. Furthermore, only K/Mn ratio excesses certain amount (H6/400), samples keep amorphous (Fig. S2(c), Supporting information).

The TG/DSC plots of H2 and K12 sample are shown in Fig. S1 (Supporting information). The progressive weight loss from room temperature to 500 °C is observed, which is due to removal of physical adsorption and dehydroxylation water. Sudden weight loss is observed at around 850 °C both for H2 and K12, which are due to generation of $Mn_2O_3$ (JCPDS. No. 24-0508) for H2 and of $Mn_3O_4$ (JCPDS. No. 24-0734) for K12. Unlike H2 first converts to $Mn_2O_3$ and then deoxygenates to $Mn_3O_4$ (Fig. 1(c)), K12 converts to $Mn_3O_4$ from $MnO_2$ directly without $Mn_2O_3$. A new phase of birnessite-type $MnO_2$ (JCPDS. No. 42-1317) appears after K12 is annealed at 900 °C (Fig. 1(d)), but it becomes pure $Mn_3O_4$ when the annealing temperature raised to 1000 °C.

The XPS spectra of as-prepared samples clearly show that from H2 to K12, the amount of K ion increases gradually (Fig. S3, Supporting information), which is in agree with the ICP result (Tables 1 and 2, Supporting information).

Based on the results of Fig. 1 and Fig. S1, it can be inferred that the crystallinity decreases gradually with the increase of K ions from K8 to K12, and the phase transition temperature is also changed. Without adding $K^+$, H2 became α-$MnO_2$ with good crystalline state after annealing at 400 °C in air, while K12 sample still maintains poorly crystalline forms up to 600 °C (Fig. S2, Supporting

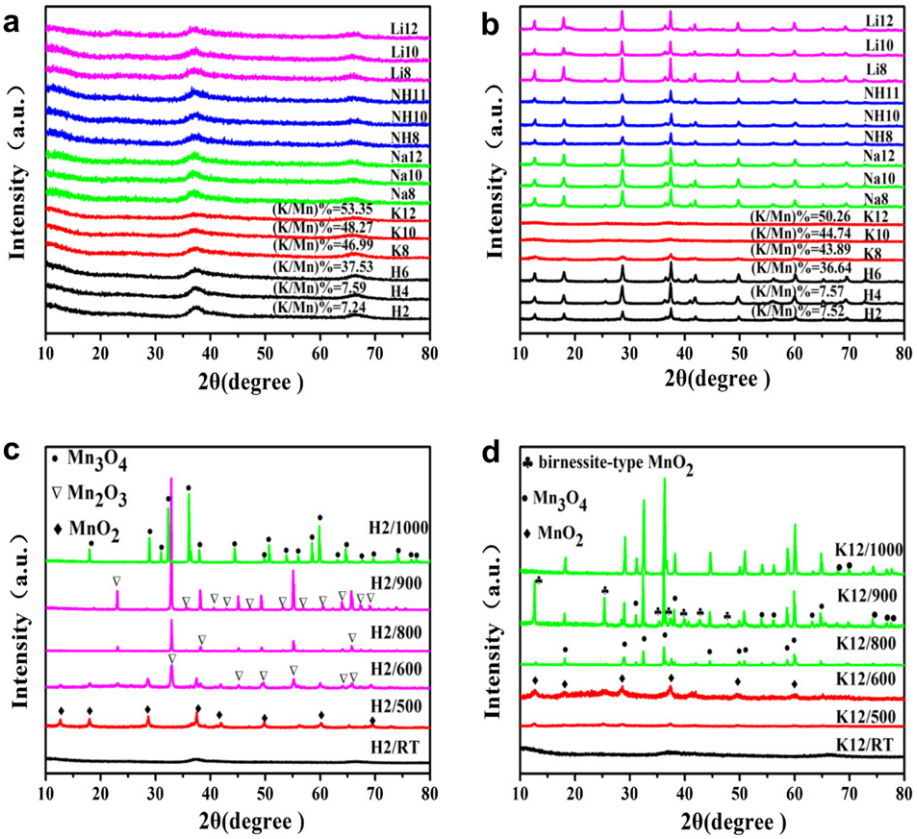


**Fig. 1.** XRD patterns of as-synthesized $MnO_2$: (a) room temperature; (b) annealed at 400 °C for 4 h; (c, d) H2 and K12 annealed at different temperature in air for 4 h.

information). As $K^+$ is of the ideal dimension to fit the $2 \times 2$ tunnels (4.6 Å) for α-$MnO_2$, [18,19] this big difference could be ascribed to different amounts of K ion in their tunnels.

Along with the crystallinity evolution during heat treatment, the morphology of the as-prepared $MnO_2$ powders changes significantly. Fig. 2 shows the surface morphologies of as-prepared $MnO_2$ after annealed at 400 °C for 4 h. It can be seen that the $MnO_2$ are composed by aggregates of spherical nanoparticles and nanorods. The diameter of nanospheres is about 20 nm, and the size of the nanorods is about 50–100 nm in length and 50 nm in diameter. With the increase of the content of K ion from H2/400 (Fig. 2(a)) to H6/400 (Fig. 2(c)), the spherical nanoparticles disappear gradually, accompanied by the growth of nanorods of tens of nanometers in length become more and more. And with the content of K ion increased continually, there are more nanorods about 20 nm in diameters and hundreds of nanometers in length (Fig. 3(d–f)). Therefore, it is concluded that the K ion promotes the nanorods growth.

Fig. 3 shows great difference after the as-prepared samples are annealed at 400 °C for 4 h. It can be clearly seen that H2, H4, H6 and K8 show good crystalline, while K10 and K12 keep amorphous state, this is in accord with Fig. S2 (see Supporting information). With the increase of $K^+$ concentration, the $MnO_2$ nanostructures change from highly crystalline to amorphous accordingly.

In order to fully understand the big difference between the morphology and crystallinity which are caused by the content of K ion, nitrogen adsorption and desorption analyses of $MnO_2$ samples are measured and the results are given in Fig. S4(a) (see Supporting information). The isotherms of H2/400, H4/400, and H6/400 belong to type IV, which is typical for a mesoporous material with a hysteresis loop. Alternatively, the isotherms of K8/400, K10/400, and K12/400 belong to type II, which has a characteristic feature of nonporous solids. Although H2/400, H4/400, and H6/400 exhibit the same type of adsorption–desorption isotherm, their surface and pore size distribution are different. Fig. 4(b) (Supporting information) shows the pore size distribution of the six samples calculated by using the BJH method. The specific surface area is calculated by using the BET equation, surface and pore characteristics are summarized in Table 3 (Supporting information). It is clearly shown that with the content of K ion increasing, the $S_{BET}$ value of samples decreases drastically from 139.6 $m^2\ g^{-1}$ for H2/400 to 4.5 $m^2\ g^{-1}$ for K12/400, and pore volume is getting smaller from 0.319 $cm^3\ g^{-1}$ (H2/400) to 0.008 $cm^3\ g^{-1}$ (K12/400). The total pore volume of H2/400, H4/400 and H6/400 are larger than those of K8/400, K10/400 and K12/400, respectively. These differences indicate that H2/400, H4/400 and H6/400 are more porous than K8/400, K10/400 and K12/400.

To explore the potential applications of the $MnO_2$ with different content of K ion, the as-prepared samples were fabricated into the supercapacitor electrode. Electrochemical measurements of the performance of electrodes, were conducted in 0.1 M $Na_2SO_4$

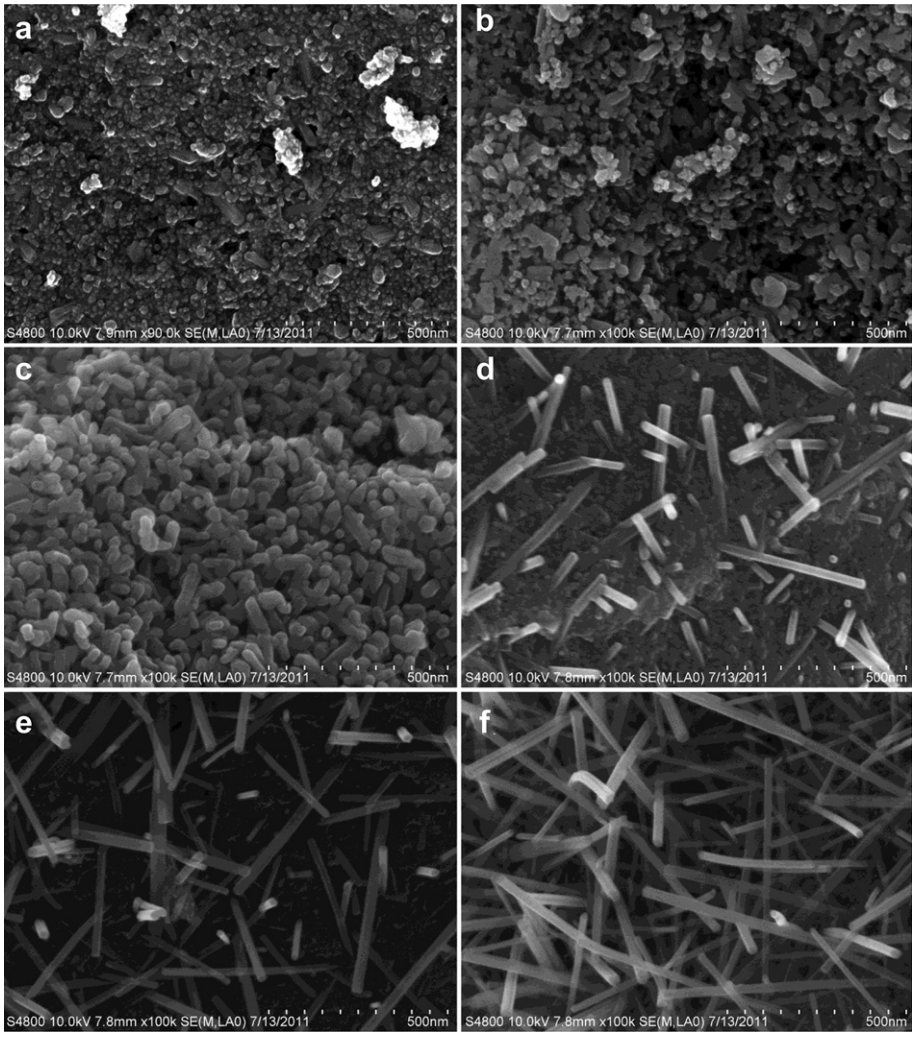


**Fig. 2.** SEM images of as-synthesized $MnO_2$ annealed in air at 400 °C for 4 h: (a) H2/400, (b) H4/400, (c) H6/400, (d) K8/400, (e) K10/400, and (f) K12/400.

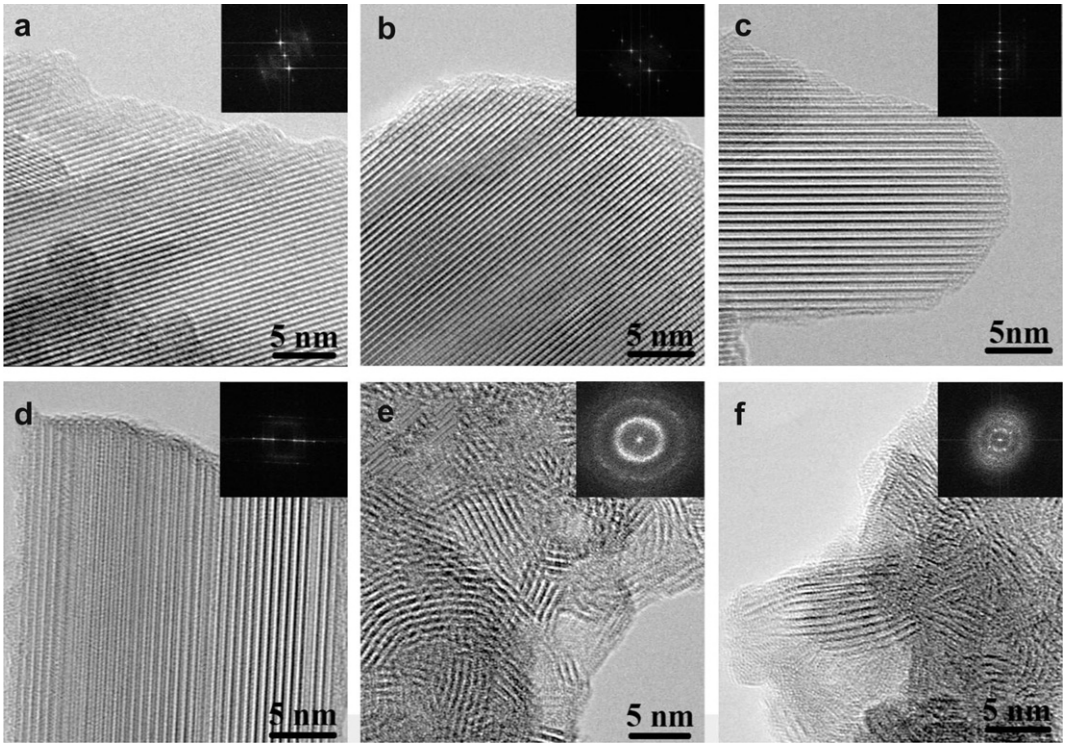


**Fig. 3.** HRTEM images of as-synthesized $MnO_2$: (a) H2/400, (b) H4/400, (c) H6/400, (d) K8/400, (e) K10/400, and (f) K12/400.

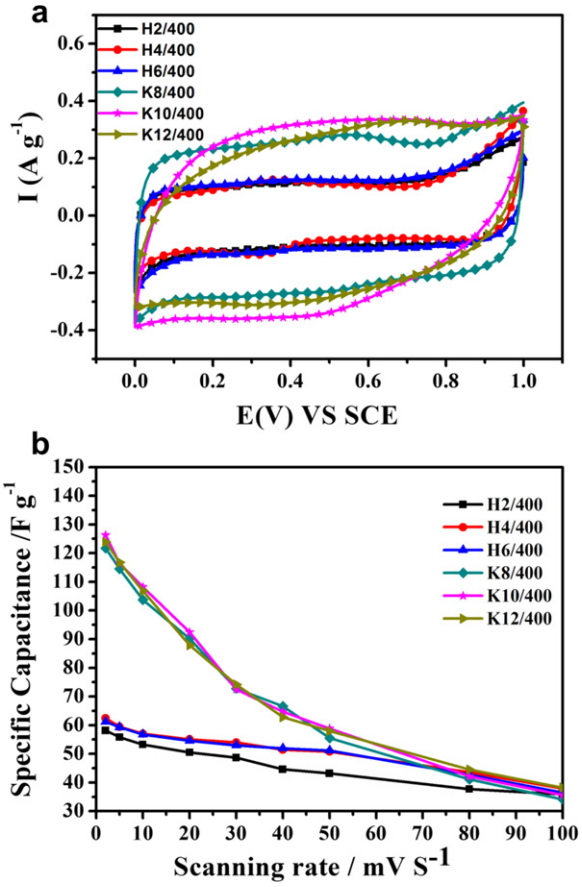


**Fig. 4.** Cyclic voltammograms of samples recorded between 0 and 1.0 V vs SCE in 0.1 M $Na_2SO_4$ aqueous solution: (a) at a sweep rate of 2 mV $s^{-1}$; (b) dependence of SC on scanning rate.

aqueous electrolyte. Fig. 4 shows the CV curves of the samples. It is noticed that the curves are symmetric closely to rectangular in shape, indicating ideal capacitance behavior of reversible reaction. A decrease in specific capacitance (SC) value with increasing sweep rate is observed for all samples, implying the decrease in the utilization efficiency of the active materials at high sweep rate. The big difference of SC value is mainly attributed to the crystallinity of the samples. It is reported that the amorphous α-$MnO_2$ has the biggest SC value during a wide diversity of crystal forms [1]. The K8/400, K10/400 and K12/400 are amorphous α-$MnO_2$ (Fig. S2(c) Supporting information), while H2/400, H4/400, and H6/400 are crystal α-$MnO_2$. Therefore, the SC value of the as-prepared samples increases from 58 F $g^{-1}$ for H2/400 to 124 F $g^{-1}$ for K12/400.

In summary, the $Li^+$, $Na^+$, $K^+$, $NH_4^+$, or $H_3O^+$ is required to stabilize the tunnels in the formation of $MnO_2$, only K ion has the anomalous effect on $MnO_2$ crystalline state. In order to investigate the effect of the content of K ion on amorphous $MnO_2$ crystalline performance, samples with different $K^+$ concentration are synthesized. It is found that the concentration of K ion not only delays the conversion of manganese dioxide crystalline, but also delays the phase transformation temperature (Fig. S1, Supporting information). Furthermore, the K/Mn ratio of samples is almost unchanged at room temperature and after annealing in air at 400 °C for 4 h, only K/Mn ratio excesses certain amount (H6/400), the amorphous state can be maintained. The K8/600, K10/600 and K12/600 are still poorly in crystalline state of α-$MnO_2$ (JCPDS. No. 44-0141), while H2, H4 and H6 become well crystalline state at 400 °C, which caused the big difference of SC value from 58 F $g^{-1}$ for H2/400 to 124 F $g^{-1}$ for K12/400. These results have important implications for the characterization of $MnO_2$ in supercapacitor applications.

## Acknowledgment

We like to thank the financial support from National Nature Science Foundation of China under Grants (No. 51102139 and No.

50972065). We also thank the financial support from Guangdong Province Innovation R&D Team Plan (No. 2009010025) and from China Postdoctoral Science Foundation (No. 2012M510022).

## Appendix A. Supporting information

Supplementary data related to this article can be found at http://dx.doi.org/10.1016/j.jpowsour.2012.09.076.

## References

[1] S. Devaraj, N. Munichandraiah, J. Phys. Chem. C 112 (2008) 4406–4417.
[2] L.C. Zhang, Z.H. Liu, H. Lv, X.H. Tang, K. Ooi, J. Phys. Chem. C 111 (2007) 8418–8423.
[3] J.T. Zhang, W. Chu, J.W. Jiang, X.S. Zhao, Nanotechnology 22 (2011) 125703.
[4] S. Chen, J.W. Zhu, X.D. Wu, Q.F. Han, X. Wang, ACS Nano 4 (2010) 2822–2830.
[5] Y.S. Ding, X.F. Shen, S. Gomez, H. Luo, M. Aindow, S.L. Suib, Adv. Funct. Mater. 16 (2006) 549–555.
[6] J.B. Fei, Y. Cui, X.H. Yan, W. Qi, Y. Yang, K.W. Wang, Q. He, J.B. Li, Adv. Mater. 20 (2008) 452–456.
[7] A.E. Fischer, K.A. Pettigrew, D.R. Rolison, R.M. Stroud, J.W. Long, Nano Lett. 7 (2007) 281–286.
[8] M. Wei, Y. Konishi, H. Zhou, H. Sugihara, H. Arakawa, Nanotechnology 16 (2005) 245–249.
[9] Q. Feng, K. Yanagisawa, N. Yamasaki, J. Porous Mater. 5 (1998) 153–161.
[10] M.M. Thackeray, Prog. Solid State Chem. 25 (1997) 1–71.
[11] O. Ghodbane, J.L. Pascal, F. Favier, ACS Appl. Mater. Interfaces 1 (2009) 1130–1139.
[12] S.L. Brock, M. Sanabria, S.L. Suib, V. Urban, P. Thiyagarajan, D.I. Potter, J. Phys. Chem. B 103 (1999) 7416–7428.
[13] Q. Feng, H. Kanoh, K. Ooi, J. Mater. Chem. 9 (1999) 319–333.
[14] P. Simon, Y. Gogotsi, Nat. Mater. 7 (2008) 845–854.
[15] S.L. Suib, Acc. Chem. Res. 41 (2008) 479–487.
[16] X.H. Tang, H.J. Li, Z.H. Liu, Z.P. Yang, Z.L. Wang, J. Power Sources 196 (2011) 855–859.
[17] T. Brousse, M. Toupin, R. Dugas, L. Athouel, O. Crosnier, D. Belanger, J. Electrochem. Soc. 153 (2006) A2171–A2180.
[18] S.L. Brock, N.G. Duan, Z.R. Tian, O. Giraldo, H. Zhou, S.L. Suib, Chem. Mater. 10 (1998) 2619–2628.
[19] R.N. Reddy, R.G. Reddy, J. Power Sources 124 (2003) 330–337.
[20] J. Luo, H.T. Zhu, H.M. Fan, J.K. Liang, H.L. Shi, G.H. Rao, J.B. Li, Z.M. Du, Z.X. Shen, J. Phys. Chem. C 112 (2008) 12594–12598.
[21] X.F. Xie, L. Gao, Carbon 45 (2007) 2365–2373.
[22] X. Wang, Y.D. Li, Chem. Commun. (2002) 764–765.
[23] C.L. Xu, Y.Q. Zhao, G.W. Yang, F.S. Li, H.L. Li, Chem. Commun. (2009) 7575–7577.